



Development of green electrode process technology for high power lithium-ion battery

Abhay Kumar Mahanta*, Prerana Priyadarshini, Navneet Kumar, and T. V. S. L. Satyavani

Naval Science & Technological Laboratory, Defence Research & Development Organization (DRDO), Visakhapatnam, Andhra Pradesh, India.

Abstract: The present work reports on fabrication and electrochemical evaluation of LiFePO_4/C based composite electrode for lithium ion battery using aqueous medium with carboxymethyl cellulose and citric acid as biomass derived sustainable binder materials. The composite electrode was prepared by dispersing the LiFePO_4/C and acetylene black powders in aqueous suspension of carboxymethyl cellulose and citric acid with fractional weight ratio of 80:10:10 (w/w %). The carboxymethyl cellulose with citric acid additive significantly improved the cyclic performance of the composite cathode with specific capacity of 85 mAhg^{-1} and 65 mAhg^{-1} at 4 C and 5 C-rates respectively and good capacity retention with 100 mAhg^{-1} after 50 cycles at 1 C discharge rate. The improved performance was attributed to good adhesion and excellent dispersion of particles within the composite electrode. This work demonstrated that switching to water based production process could reduce the manufacturing cost significantly with additional advantage of safety, performance, and more importantly environmental benign electrodes for lithium ion battery.

Keywords: Green electrode, carboxymethyl cellulose, citric acid, LFP, lithium ion battery.

1 Introduction: Apart from consumer electronics, lithium ion battery technology is emerging as a technology of choice for military, electric vehicles, and aerospace applications. For example, it can be used to power AUV, SAT, Drones, UAV, HEV, EV, Satellites, etc. The global market of lithium ion batteries is estimated to be 10 billion dollars and predicted to grow 60 billion dollars by 2020 [1-3]. In the coming years, India is expected to witness substantial investments made by industries in setting up indigenous Li-ion battery manufacturing base in the country. The present demands, therefore, stimulate for development of advanced lithium ion battery technology capable of improving power density, cycle life, charge/discharge rates, and design flexibility with low cost, environment benignity, and higher safety margin as compared to conventional technology.

The conventional Li-ion battery technology depends upon substantial use of battery components that are far from renewable and sustainable energy sources [4]. For example, fabrication of composite electrode requires a synthetic polymer, *i.e.* polyvinylidene difluoride (PVDF) which uses N-methyl-2-pyrrolidone (NMP) as solvent during electrode processing. NMP is a heterocyclic liquid and volatile organic compound (VOC) with boiling point of 200°C . It is classified by the European Union as toxic that imposes many health and environmental hazards [5, 6]. PVDF solution is highly sensitive to moisture in air, therefore requires stringent humidity control environment for electrode processing. Apart from this, it reacts with lithium metal as well as lithiated graphite (anode) exothermally at elevated temperature, and makes the battery unsafe imposing a high risk of fire and explosion hazards [4]. Further, the cost of

PVDF is very high due to the complicated synthesis and expensive monomer used, and along with the highly priced NMP-solvent, it raises the cost of the battery manifold. Therefore, to sustain the Li-ion battery technology, there is an urgent need to address the various issues through green technology which is based upon 12-principles (Figure (1)) [7].

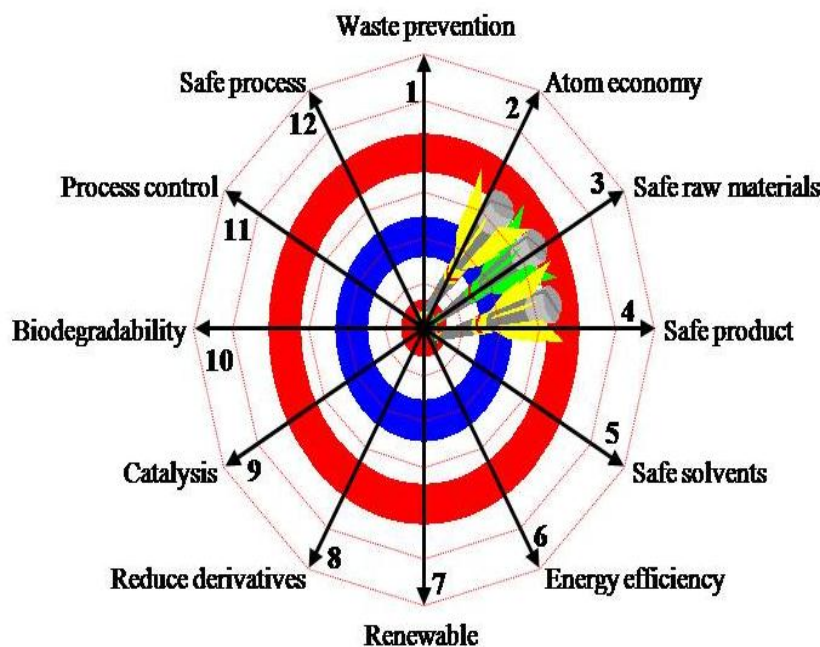


Figure (1): 12-Principles of green technology.

Following the principle of green technology, one of the alternative solutions to PVDF based composite electrodes for lithium ion batteries (LIBs) would be to adopt the aqueous processing (safe solvent) of the composite electrodes. Aqueous route provides cleaner and safer working environment while administering economic benefits to industries [8]. It is an extremely promising approach providing a pathway to reduced cost in which the expensive NMP (Rs.1700/L) is replaced with de-ionized water (Rs.30/L). Some biomass derived aqueous polymers used in lithium ion battery fabrication are shown in Figure (2).

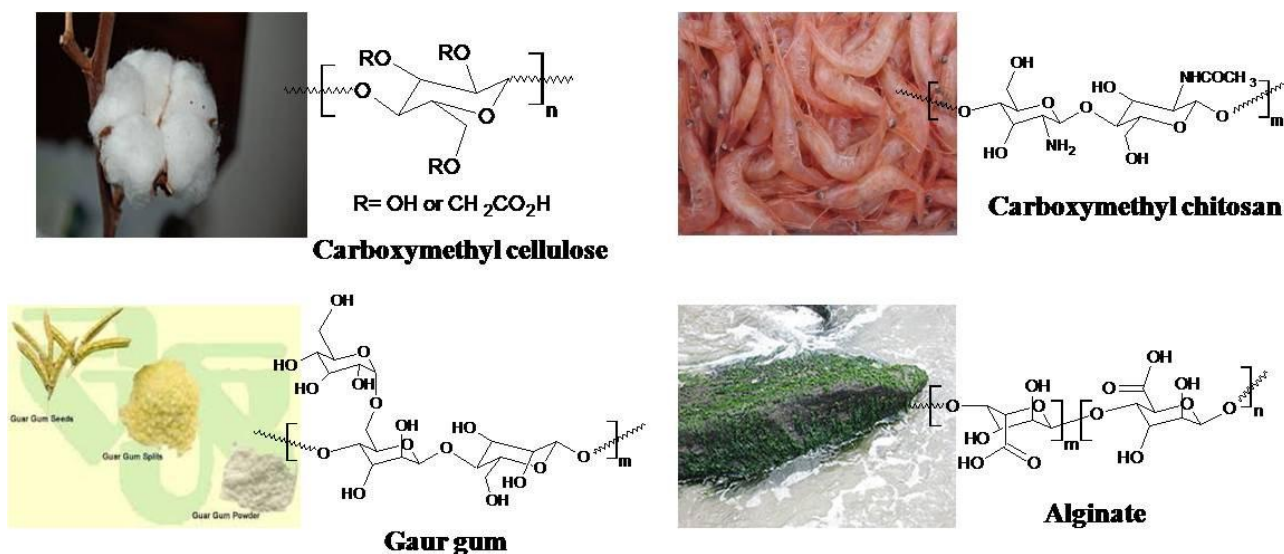


Figure (2). Chemical structures of some biomass derived binders for Li-ion battery.

Carboxymethyl cellulose (CMC), alginate, sodium polyacrylate (PAANa), styrene-butadiene rubber (SBR), carboxymethyl chitosan (C-CTS), pectin, xanthan gum, carbonyl- β -cyclodextrin, amylopectin, lignin, gaur gum, catechol-conjugated alginate, polyvinyl alcohol, poly(acrylic acid sodium)-g-CMC have recently been explored to serve as robust and green binders to overcome the limitation of PVDF based binder systems for Li-ion electrode fabrication [4, 9-13].

The objective of the work is to apply environmentally and economically sustainable concepts (green technology) in fabrication of green electrodes for Li-ion battery cell. After carefully screening various biomass derived binders, Na-CMC was particularly chosen because it is stable, non-flammable, hazards free, and water dispersible polymeric binder. Further, the cost is very competitive when compared to PVDF polymer. Moreover, the cathode active material selected for this work is the carbon coated lithium iron phosphate (LiFePO_4/C) which is highly stable on prolonged cycling, safe, cheap, and environmental friendly material [14-18].

2. Experimental

2.1 Materials and Equipment: LiFePO_4/C powder was obtained from Targray. Na-CMC was purchased from Sigma-Aldrich, India. The electrolyte of 1M LiPF_6 in ethylene carbonate (EC, > 99.9 %), diethyl carbonate (DEC, > 99.9 %), dimethyl carbonate (DMC, > 99.9 %) in 1:1:1, ratio (v/v) was purchased from Targray India with water content < 20 ppm. De-ionized water was purchased from the local market and used as solvent in the composite fabrication process. Charge/discharge data were obtained by multi-channel electrochemical analyzer (Ivium-n-Stat). TGA measurements were conducted on a Mettler Toledo thermal system in air atmosphere with heating rate of 5 °C/min. from room temperature to 600 °C. Viscosity was measured by Brookfield viscometer (model DV2TLV) at 30 °C using SC4-16 spindle at room temperature. Particle size distribution in dilute medium was measured by laser diffraction particle size analyzer (Microtrac S3500-Extended). For particle size analysis, Na-CMC and acetylene black samples were wetted with 5 drops of 2 % Triton X-100 surfactant in water and further dispersed in water and sonicated externally by 60 Watts probe sonicator for 10 minutes whereas LiFePO_4/C was directly measured in water medium. The surface weight and the film thickness of the dried electrode were measured, and both values together with the mean density of the dry layer were used to estimate the electrode porosity. The adhesion of the electrode layer to the current collector was investigated by 180 degree peel test using Housfield UTM-H25KS. Electrode layers with a width of 25 mm and a length of 40 mm were investigated by peel testing at preselected peel velocity and the resulting peel force was measured. The peel velocity had negligible influence on the measured peel force and therefore, it was kept constant at 5 mm/min. A 100 N load cell force sensor was applied for all the peel test measurements.

2.2 Preparation of Composite Slurry and Electrode: Active material (LFP), acetylene black powder as conducting agent, and the aqueous binder (Na-CMC) were mixed by a mechanical mixer at a ratio of x:y:z (by weight) in de-ionized water to a required slurry viscosity. The composition was optimized to 80:10:10 ratio of active material, acetylene black and binder by varying the formulations. The raw material addition sequence and mixing time were established by varying the process parameters systematically. The composite slurry was prepared as follows: at first the binder solution was prepared by mixing the powdered CMC in water along with citric acid at 40 °C for 1 hour. In the mean while, dry mixing was carried out with LiFePO_4/C and carbon black for about 30 minutes to remove agglomerates. After 1-hour mixing of binder solution, the dry mixed materials were added in four installments for the preparation of the slurry. Then, the mixing was continued for about 3 hours. The slurry was taken out and pH was measured using pH meter. Some part of it was taken for rheology studies, and the remaining quantity was used for coating the electrode sheets. The slurry was cast on 18 μm thickness aluminum current collector with the help of a doctor blade at a speed of 15 mm/s. Electrode coating was carried out

with wet thickness ranging from 150 μm to 300 μm . After casting, the electrode sheets were dried under vacuum at 80 $^{\circ}\text{C}$ for 12 h. Circular electrodes were punched out with an area of 1.77 cm^2 and a loading of 3-7 mg/cm^2 . Before assembly, the electrodes were dried for 12 h at 110 $^{\circ}\text{C}$ under vacuum to remove the residual water from the composite electrode.

2.3 Electrochemical Performance Studies of Composite Cathode: Coin cells (CR2032) were tested to evaluate the electrochemical performance of the composite cathodes. The cells were assembled in a glove box filled with argon gas. A micro-porous tri-layer polymeric membrane (polypropylene-polyethylene- polypropylene) was used as a separator. The electrolyte was one molar of LiPF_6 solution in ethylene carbonate: dimethyl carbonate: diethyl carbonate (1:1:1, v/v). Pure lithium metal was employed as anode. The charge/discharge cycling was galvanostatically performed at different current density (0.05 to 5 C rates) within the cut-off voltage of the electrode at room temperature in a multi-channel battery tester. 1 C current was calculated according to the theoretical capacity of the active material. All capacity values were normalized by the total weight of electro-active material present in various formulations.

3. Results and Discussion:

3.1 Characterization of Battery Raw Materials:

The performance of lithium ion battery is governed by the choice of materials used in manufacturing of the battery electrodes. The shape and size of the particles that make up the Li-ion battery electrodes have a significant impact on the final performance of the electrodes in terms of packing density, porosity, Li-ion diffusion, and intercalation properties. In order to obtain high energy and high power characteristics in the Li-ion battery, particle size and size distribution of electrode's raw materials need to be carefully controlled within the set parameters. It is quite feasible to tune the electrode materials in order to achieve a high energy density or high power depending on their particle size distribution. Studies have shown that a poly-disperse distribution of particles can provide up to twice the energy density than that of a mono-disperse particle size distribution whereas a mono-disperse particle distribution produces a higher power density at high discharge rates. In Li-ion battery, primary particles are controlled in the range from 20 nm to 300 nm in size and the agglomerated particles in the range from 1 μm to 20 μm . Nano-structured spherical morphology with a narrow size distribution of primary particle size basically dictates the electrochemical performance including cycling, rate capability, and low-temperature performance [19]. The particle size of the battery raw materials was measured by laser diffraction particle size analyzer. Figure (3) shows the particle size distribution of LiFePO_4/C , acetylene black, and carboxymethyl cellulose dispersed in water.

Table (1). Particle size distribution of various battery raw materials.

Ingredients of Electrode	Values in μm			
	D10	D50	D90	Mean Value
Acetylene black	0.14	0.92	4.05	0.877
LiFePO_4/C	1.85	4.58	10.67	5.74
Carboxymethyl cellulose	7.85	27.56	92.20	42.02

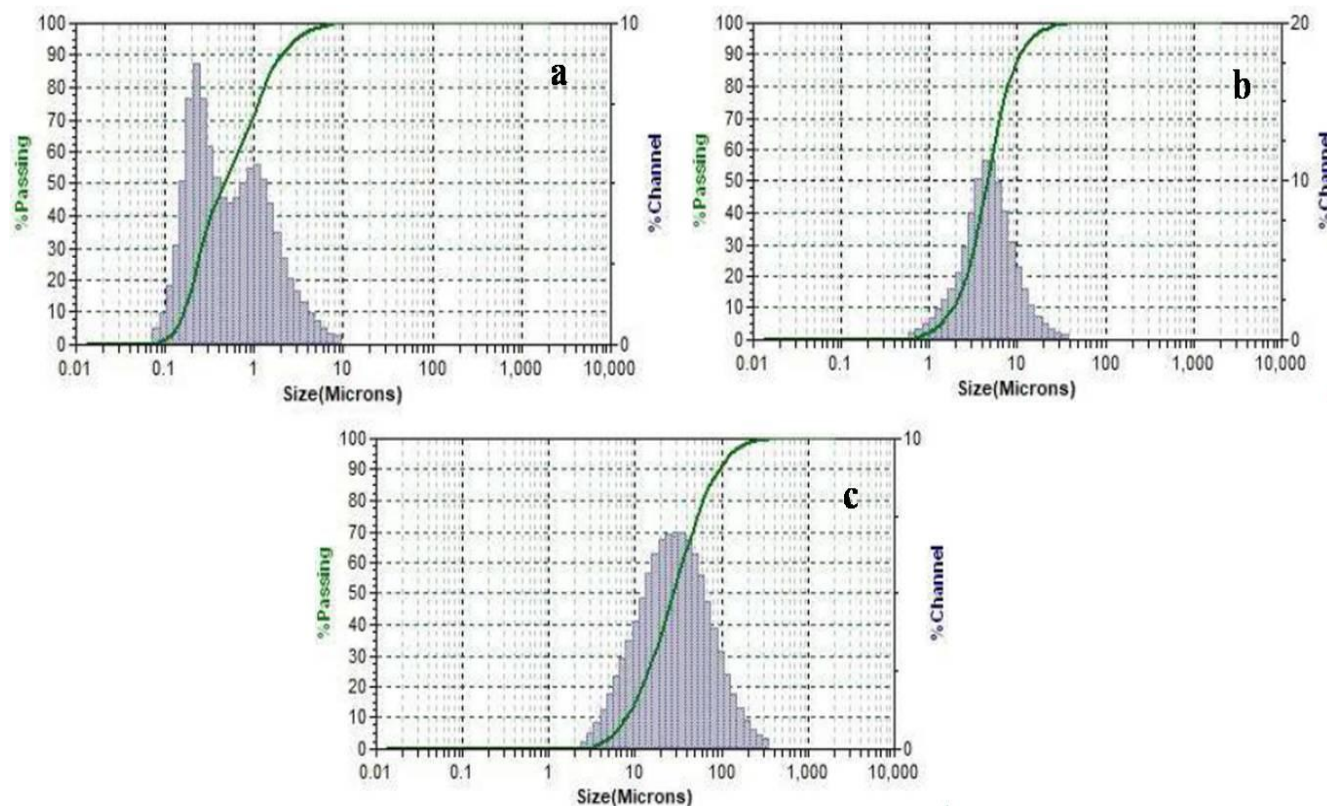


Figure (3). Particle size distribution of (a) Acetylene black, (b) LiFePO₄/C, and (c) Na-CMC.

It could be seen that acetylene black distributed between two populations, one nano-metric and the other micro-metric. The micro-metric population is centered at 1 μm with average particle size of 0.877 μm . For LiFePO₄/C, most of the micro-metric particles are distributed from 1 to 12 μm and centered on 8 μm with average size of 5.74 μm , whereas the binder particle distribution ranges from 5 to 500 μm with average size being 42.02 μm . The details particle size distribution is provided in Table (1).

Figure (4)-(a) shows the FTIR spectrum of Na-CMC. FTIR showed the absorption bands of the cellulose backbone as well as the presence of carboxy-methyl substituent in Na-CMC. The broad band above 3500 cm^{-1} was attributed to the stretching frequency of -OH groups and inter-molecular and intra-molecular hydrogen bonds. The band at 2841-3043 cm^{-1} is attributed to -CH stretching vibration. The carboxyl group and its salt show two peaks in the range 1600-1650 cm^{-1} and 1400–1450 cm^{-1} indicating the presence of carboxy-methyl substituent in Na-CMC. While another proof of cellulose backbone is the absorption bands at 1425 cm^{-1} and 1327 cm^{-1} which are assigned to -CH₂ scissoring and -OH bending vibration, respectively. The -C-O-C-glycosidic ether band appeared at 902-1020 cm^{-1} [20].

The functional groups of acetylene black are characterized by FTIR spectroscopy and shown in Figure (4)-(b). The characteristic peak observed above 3500 cm^{-1} is attributed to -OH stretching vibration from water absorption or hydroxyl group present in the material. The small peaks at 2945 and 2872 cm^{-1} are due to asymmetric and symmetric stretching vibrations of -C-H bond. The peaks at 1612, 1204, and 991 cm^{-1} could be attributed to the stretching vibration of -C=C-, -C-O-, and plane deformation vibration of -C-H bonds.

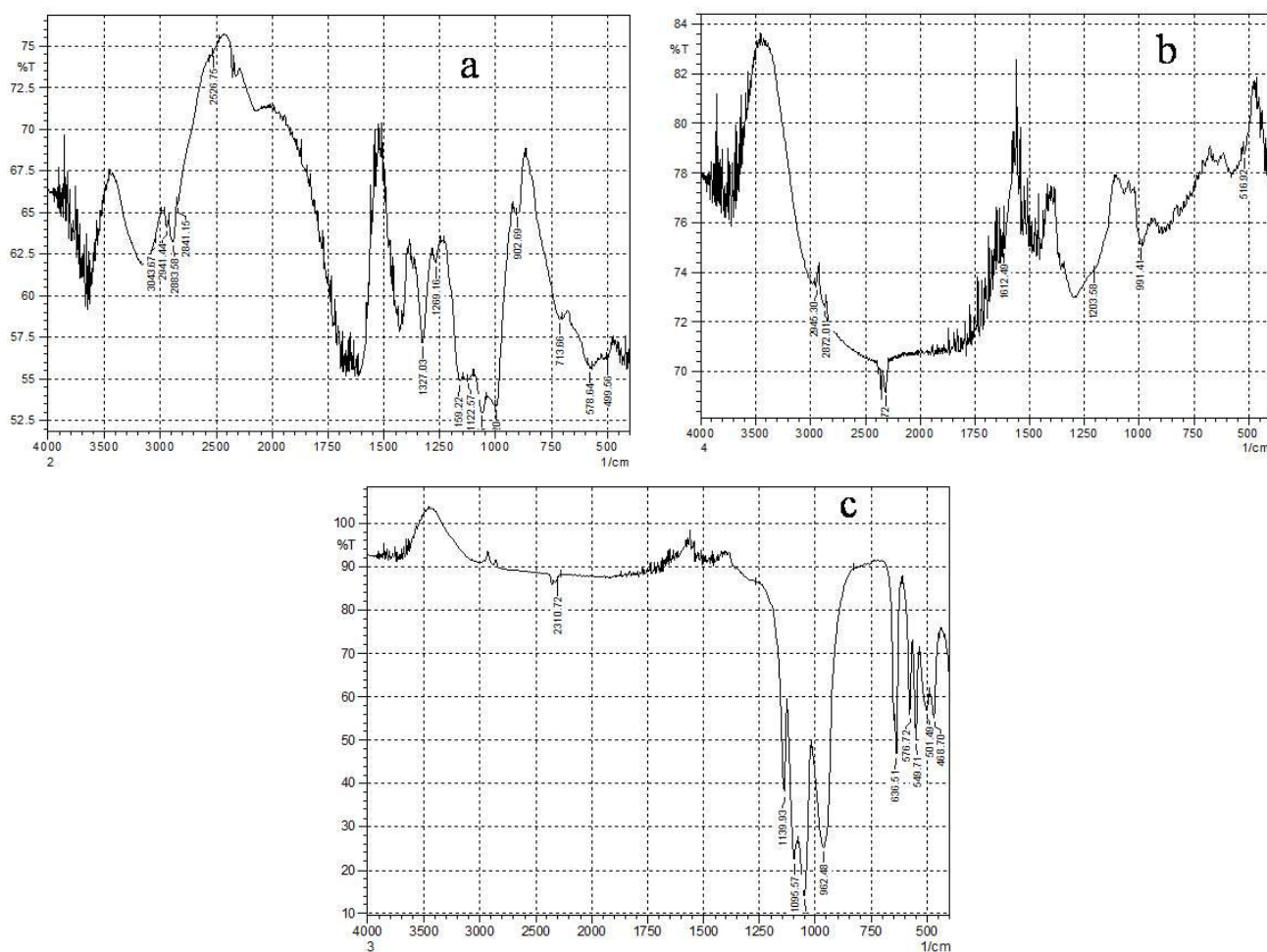


Figure (4): FTIR spectrum of (a) Na-CMC polymer, (b) acetylene black, and (c) LiFePO_4 active material. (X-axis represents the wavelength (cm^{-1}) and Y-axis represents light transmittance through the sample).

The FTIR spectrum of LiFePO_4 is shown in Figure (4)-(c). It could be seen that the absorption bands are mainly distributed over two wavenumber ranges. The high wavenumber domain ($600\text{--}1140\text{ cm}^{-1}$) is due to stretching vibrations and the low wavenumber domain ($300\text{--}600\text{ cm}^{-1}$) corresponds to bending modes of P-O vibration. The band at $469\text{--}500\text{ cm}^{-1}$ is due to anti-symmetric P-O bending modes. The band at $500\text{--}637\text{ cm}^{-1}$ is due to intra-molecular symmetrical stretching vibrations of the Fe-O bond in the FeO_6 unit. The bands located in the high wave number region from 600 to 1140 cm^{-1} are due to internal modes corresponding to the intra-molecular vibrations of the $(\text{PO}_4)^{3-}$ oxyanion. The dominant bands at 962 , 1096 and 1140 cm^{-1} are assigned to the P-O stretching mode. The band at 2311 cm^{-1} is due to the symmetric P-O stretching vibration. As mentioned that LFP particle's surface is coated with carbon, the surface of the LFP particle was found to be composed with two parts. Surface of LFP particles is partially covered with metallic component, which was confirmed by P-O/Fe-O stretch peaks. Also we could see that the remaining portion of LFP surface, covered with carbon, had similar surface properties with that of acetylene black. FTIR spectra therefore confirmed that carbon was coated on the surface of the LiFePO_4 particles and in good agreement with those of the LiFePO_4 olivine. It gives no evidence to any impurity phase [21].

The TGA curve for Na-CMC is shown in Figure (5). The weight loss below 100°C (first step, about 10 %) is attributed to the evaporation of adsorbed moisture. The weight loss from 250 to 310°C , with a

maximum degradation peak at 280 °C (second step, about 38 %) followed by a smooth degradation (third step, about 11 %) is attributed to de-carboxylation and decomposition of Na-CMC and formation of carbonaceous char. This good thermal stability of the polymer ensured that it could be used as a polymeric binder in fabrication of composite cathode. The fabrication process of composite cathodes hardly exceeds 150 °C.

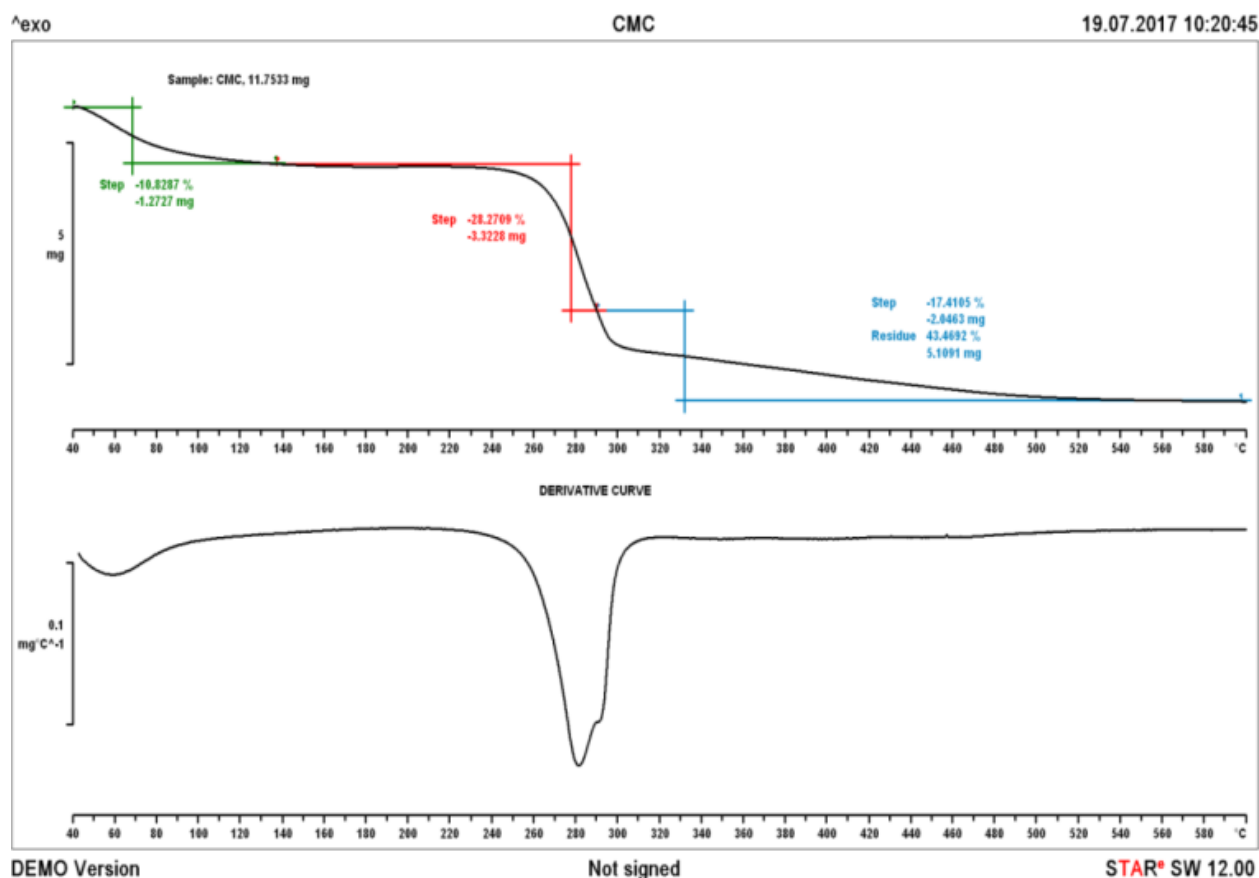


Figure (5). TGA analysis of Na-CMC at 5 °C/min. in air atmosphere

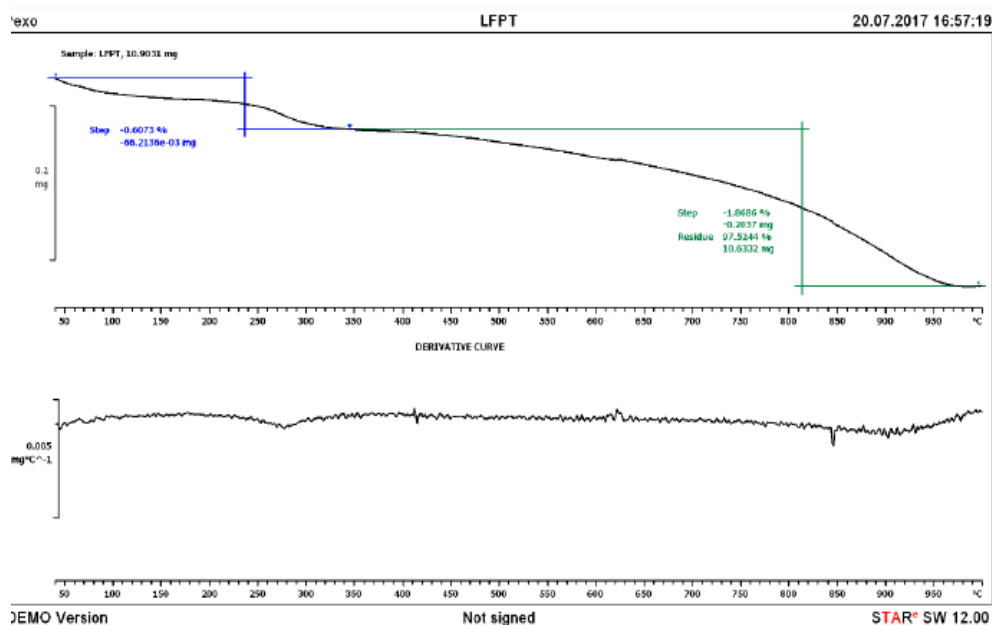


Figure (6). TGA analysis of LFePO₄/C at 5 °C/min. in air atmosphere

The DTA/TG result of LiFePO_4/C is shown in Figure (6). The weight loss at temperature between 60 and 300 °C is due to water evaporation [21]. The weight loss in the temperature range of 600-950 °C is due to carbon oxidation to CO_2 in LiFePO_4 . No prominent oxidation peak was observed in the range of 300-510 °C indicating that carbon coating protected well the LiFePO_4 crystal from oxidative reactions.

3.2 Rheological Properties of the Composite Slurry:

The high viscosity at low shear rates improves the coating process in terms of obtaining better layers on the current collector and therefore reducing the cost by avoiding cut-off waste. A fluid with a high viscosity at low shear rates and low viscosity at high shear rates is easier to mix and it maintains uniform dispersion of the particles. The mixing time and addition sequences of the raw materials were optimized for the composite formulation. To improve the quality of coating on the current collector and improved electrochemical performance, the rheological behavior of the composite slurry was evaluated by Brookfield viscometer at 30 °C using SC4-16 spindle. Figure (7) shows the effect of shear rate on viscosity of the composite slurry measured at 30 °C with 0.4 % citric acid and 30 % solid loading.

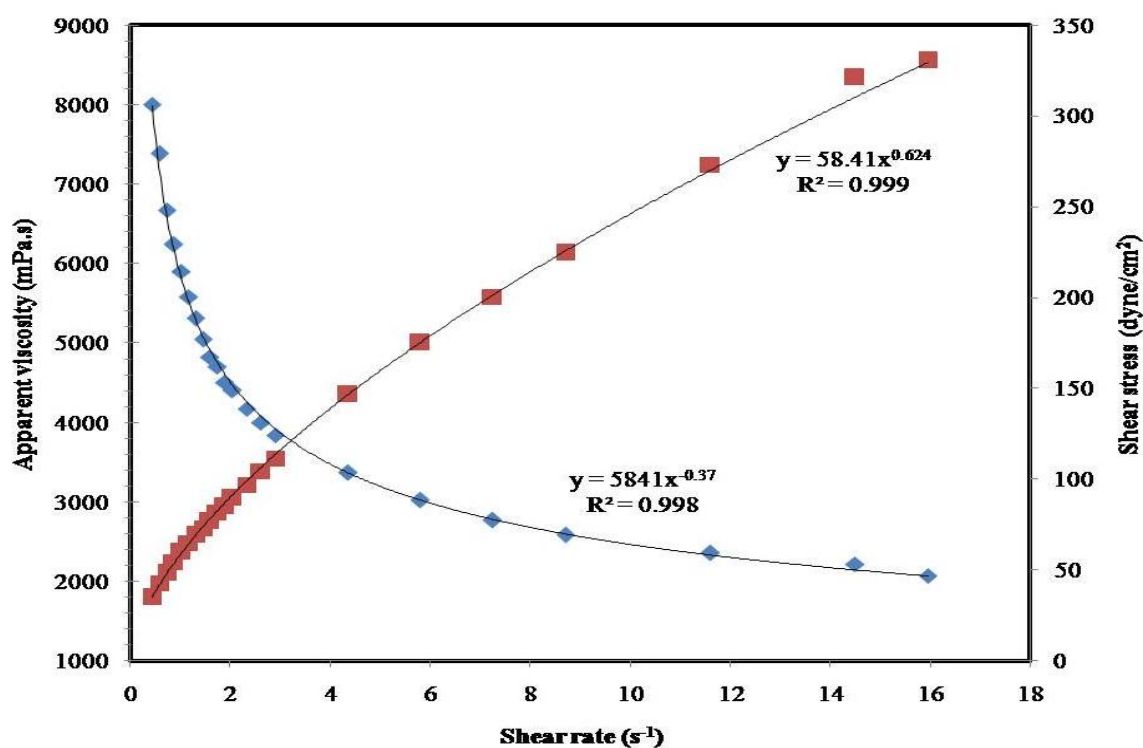


Figure (7): Effect of shear rate on viscosity and shear stress of the cathode formulation with 0.4 % citric acid and 30 % solid loading.

It was observed that viscosity of the slurry decreased with increase in shearing rates indicating non-Newtonian characteristic. The composite slurry was found to be shear sensitive and showed shear thinning behavior. This rheological behavior was found to be more pronounced in low shear rates. A wide variety of models have been proposed for representing the viscosity function for suspensions with varying degrees of complexity. To a first approximation, the flow curve of pseudoplastic slurry (shear thinning behavior) can be represented by Power Law, *i.e.* shear stress is proportional to the power of the rate of shear.

Mathematically, the Power Law equation can be written as:

$$\tau = K\dot{\gamma}^n \quad (1)$$

where τ is the shear stress in dynes/cm², γ is the shear rate in s⁻¹, K is the consistency coefficient (dynes/cm².secⁿ) and n is the flow behavior index. Equation (1) can be modified as:

$$\eta(\gamma) = K\gamma^m \quad (2)$$

where η is the apparent viscosity, $n - 1 = m$ is the pseudoplasticity index [23-25]. In Figure (7), it could be seen that the correlation coefficient obtained was in the order of 99.8 % which showed that the viscosity data were well fitted with the Power Law model. From Equations. (1) and (2), the flow behavior /pseudoplasticity index and consistency index were determined for different formulations and listed in Table (2). The pseudoplasticity index varied from 0.30-1.01 indicating shear thinning (pseudoplastic) behavior of the composite slurry.

It is further observed that the consistency index (K) depends upon the citric acid concentration. The value of K decreased proportionately with the increase in concentration of citric acid. Good quality of coating was obtained when consistency index was from 50000-60000 mPa.s and the pseudoplasticity index (m) was between 0.4 to 0.5.

Table (2). Rheological parameters of the cathode formulation with different concentrations of citric acid.

Cathode formulation (80:10:10)			
Citric Acid (%)	K	m	Solid loading (%)
0	38423	-0.30	20
0.1	28862	-1.01	27
0.2	18627	-0.57	27
0.3	9538	-0.46	27
0.4	5841	-0.37	30
0.5	58879	-0.47	35

3.3 Physico-chemical Properties of the Composite Cathode:

Porosity of the electrode plays a significant role in achieving high electrochemical performance particularly for high power application. To study the porosity of the composite, the thickness of the wet coating of the composite cathode was varied by using doctor blade and the final porosity of the dried cathode sheets was calculated from the theoretical and apparent density of the composite as per the following equations [5].

$$d_t = \frac{1}{\sum_{i=1}^n \frac{X_i}{d_{pi}}} \quad (3)$$

Where d_t is the theoretical density of the dense electrode (porosity 0 %), d_{pi} is the density of the component i , and X_i is the weight fraction of the component i . The density of the individual component of the composite electrode and their composition in the composite is listed in Table (3).

Table (3): Density of the components and formulation of the composite cathode.

Materials	Density & formulation of the composite cathode	
	Density (g/cm ³)	Formulation (%)
LiFePO ₄ /C	3.56	80
Acetylene Black	1.95	10
Carboxymethyl cellulose	1.59	10

The theoretical density of the composite electrode was calculated from Equation (3), and it was found to be 2.95 g/cm³. Similarly, the geometrical density can be calculated from Equation (4).

$$d_a = \frac{m_s}{v_s} \quad (4)$$

where d_a is the apparent density of the electrode, m_s is the mass of the sample, and v_s is the volume of the sample. The apparent density of the electrode calculated from Equation (4) was found to be 1.23 g/cm³. The Equation (5) was used to determine the electrode porosity.

$$P = \frac{d_t - d_a}{d_t} \times 100 \quad (5)$$

The porosities of the composite for various formulations were calculated by Equation (5) and found to be ranging from 75 % to 58 % for different formulations and wet coating thickness. It was observed that the porosity decreased with increase in concentration of citric acid as shown in Table (4).

Table (4). Porosity for different concentration of citric acid in cathode formulations.

Citric Acid (%)	Solid loading (%)	Porosity (%)
0	27	74.60
0.1	27	66.20
0.2	27	62.60
0.3	27	60.67
0.4	30	59.51
0.5	35	57.95

Another requirement for high power application is the good adhesion strength between the electrode layer and the current collector. The adhesion of the electrode layer to the current collector was investigated by 180 degree peel test using Housfield UTM-H25KS. Electrode layers with a width of 25 mm and a length of 40 mm were investigated by peel testing at peel velocity of 5 mm/min and the resulting peel force was measured. As expected samples with 0.5 % citric acid showed higher peel strength in the order of 0.452-0.532 N/cm and thus, it was used for further investigation for high power applications.

3.4 Electrochemical Characterization of the Composite Cathode:

The galvanostatic charge-discharge curves of the LFP/Li cell at C/20-rate was carried within the cut-off voltage between 2.5 and 4.0 V and the voltage vs. specific capacity profiles are shown in Figure (8).

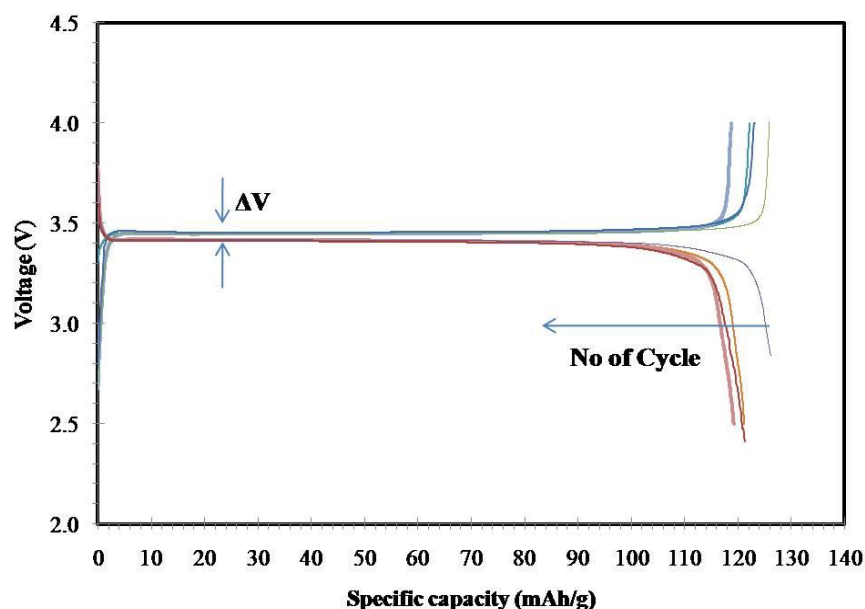


Figure (8). Specific capacity of the electrode at 0.05 C rate & 25 °C.

The capacity profiles are found to be very symmetric indicating good cycle reversibility. The discharge curve of the composite electrode exhibited a characteristic flat plateau at 3.4 V across a large capacity range indicating two phase nature of Li-ion extraction and insertion reactions between LiFePO_4/C and FePO_4/C crystals. The initial discharge capacity of the LFP/Li cell was found to be 123 mAhg^{-1} . The highest capacity which appeared in the 3rd cycle was 128 mAhg^{-1} . After 10 cycles, the discharge capacity was retained to 121 mAhg^{-1} . The slope parts at the beginning and at the end refer to the charge transfer activation and concentration polarization. The voltage difference between the flat charge and discharge plateau (ΔV) indicates the polarization of the cell. Smaller the ΔV , less will be the polarization. The ΔV values were found to be $\leq 0.1 \text{ V}$ for all the cycles, which were relatively less indicating low polarization and high performance of the LFP/Li cell.

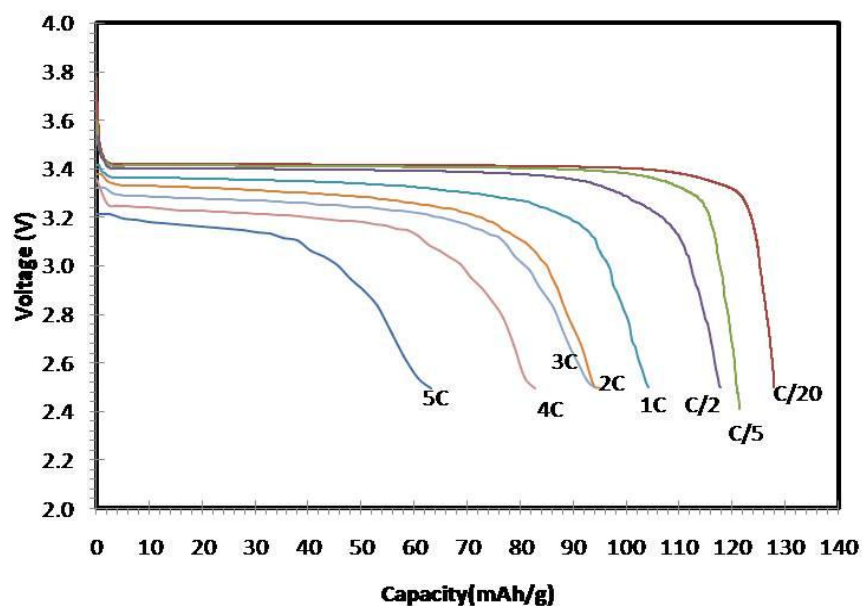


Figure (9). Rate capability of the electrode at C- rates from 0.05 C to 5 C & 25 °C.

To test the LFP/Li cell for high power application, the capacity of LFP/Li cell was discharged at higher C-rates. Figure (9) shows the discharge plots as a function of C-rates for the composite cathode. The

discharge capacity of LFP/Li cell was found to be 85 mAhg^{-1} and 65 mAhg^{-1} at 4 C and 5 C respectively. The highest capacity was achieved in the 4th cycle, i.e. 98 mAhg^{-1} at 4 C. The electrochemical results obtained in the present work were found to be comparable or even better to the conventional formulation with LiFePO_4/C (active material), acetylene black, and PVDF-HFP binder reported in the literature. For example Prosini *et al.* reported a discharge capacity of 80 mAhg^{-1} at 4 C and 40 mAhg^{-1} at 5 C for LiFePO_4/C composite cathode [5].

Figure (10) shows the discharge curves of the LFP/Li cell at 1 C before high rate discharge. The discharge capacity of LFP/Li cell was found to be 116 mAhg^{-1} . Figure (11) shows the discharge curves of the LFP/Li cell at 1 C after high rate discharge. The discharge capacity of LFP/Li cell was found to be 115 mAhg^{-1} . There was no deterioration of the composite cathode after the high rate discharge. This indicated the stability of the LFP-electrode and its potential for high power applications.

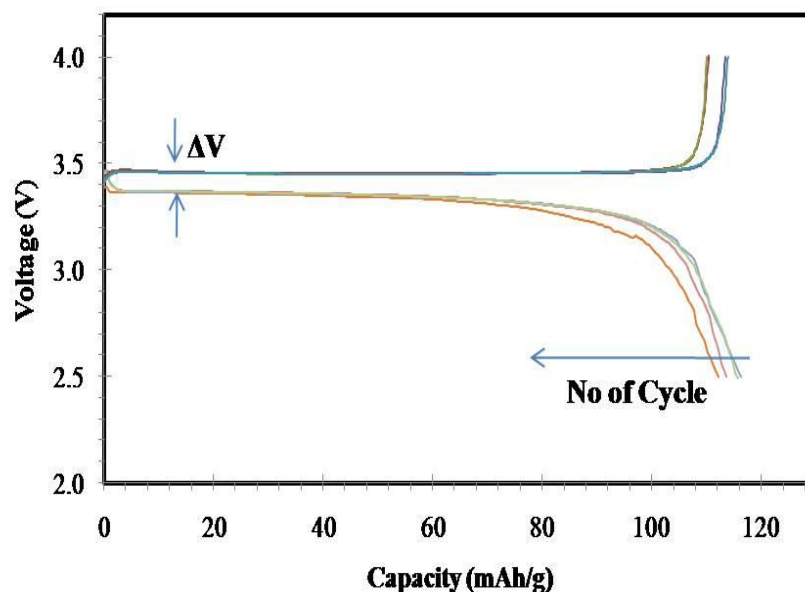


Figure (10): Specific capacity of the electrode at 1 C rate & 25 °C (before high rate discharge).

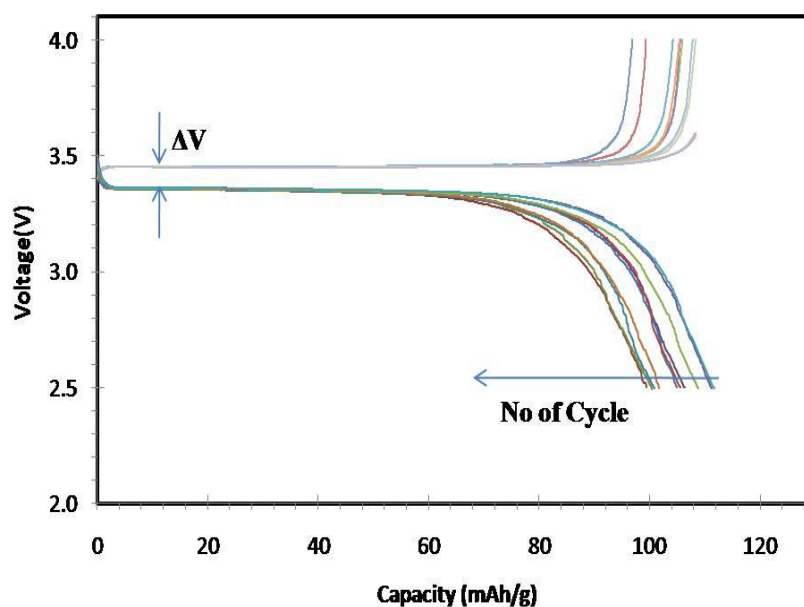


Figure (11): Specific capacity of the electrode at 1 C rate & 25 °C (after high rate discharge at 5 C).

Figure (11) also shows the discharge curves at 1 C after high discharge rate with cycle numbers. The LiFePO_4/C composite cathode was stable during extensive cycling. Moreover, it also showed appreciable capacity retention more than 85 % after the 50th charging/discharging cycles. At 50 cycle, the discharge capacity was retained at 100 mAhg^{-1} . It indicated that no unwanted side reactions occurred during charging/discharging of the composite cathode. The energy density of the cell with a discharge voltage of 3.4 V and a tap density of 1.70 kg/L was found to be 734.06 Wh/L . The results obtained in the present study are, therefore, quite remarkable in terms of long term performance and power density of the LiFePO_4/C composite cathode. Thus, it could be inferred that Na-CMC along with citric acid composite cathode improved the specific capacity of the composite and simultaneously maintained the prolonged cycle life of the composite cathode. In addition to improved electrochemical performances of the composite, it also offers the advantage of low-cost and environmental friendly water based fabrication process of the composite electrode for high power Li-ion battery applications.

4. Conclusions:

The following conclusions could be drawn from the present study of Na-CMC aqueous binder based LiFePO_4/C composite cathode for application in high power Li-ion batteries.

- The Na-CMC along with citric acid led to homogeneous dispersion of the components within the composite cathode.
- The Na-CMC with citric acid additive significantly improved the cyclic performance of the composite cathode with high specific capacity of 85 mAhg^{-1} and 65 mAhg^{-1} at 4 C and 5 C-rates respectively and good capacity retention of 100 mAhg^{-1} after 50 cycles at 1 C. As the composite cathode with the Na-CMC binder exhibited very good capacity retention on cycling, it could be considered as a promising binder material in fabrication of LiFePO_4/C composite electrode for Li-ion batteries.
- The improved electrochemical performance with the Na-CMC binder with citric acid could be attributed to the good adhesion and excellent dispersion of particles with favorable rheology. It ensures good quality of the coating on the substrate that provides uniform distribution and good electrical contact of the active particles in composite electrode leading to high lithium ion utilization.
- This work demonstrated that switching to water based production process could reduce significantly the manufacturing cost with additional advantage of safety, performance, and environmentally benign electrodes for lithium ion battery.
- The knowledge and skills gained in coin cell experiments would help in further scale-up of the composite electrode fabrication in pouch /prismatic format. The stability of cathode active material, i.e. LiFePO_4/C , in aqueous medium will be studied in detail to establish the required shelf-life of the electrode for application in high power Li-ion battery.

Acknowledgements:

Authors are thankful to Dr. A. Srinivas Kumar, Head, Batteries & Explosives Directorate of NSTL for his constant support and encouragement throughout the research work and the Director for giving permission to submit the research work for publication. We also express sincere thanks to the team members of Batteries & Explosives Directorate for their valuable support and contributions.

5. References:

- [1] D. Deng, *Eng.Sci. & Eng.* 3-5 (2015) 385.
- [2] G. Berckmans, M. Messagie, J. Smekens, N. Omar, L. Vanhaverbeke, and J. V. Mierlo, *Energies* 10 (2017) 1314.
- [3] H. Xia, Z. Luo, J. Xie, *Prog. in Nat. Sci.: Mat. Int.* 22-6 (2012) 572.

- [4] L. Zhang, Z. Liu, G. Cui, L. Chen, *Prog. in Pol. Sci.* 43 (2015) 136.
- [5] P. P. Prosini, M. Carewska, C. Cento, A. Masci, *Electrochimica Acta* 150 (2014) 129.
- [6] Z. P. Cai, Y. Liang, W. S. Li, L. D. Xing, Y. H. Liao, *J. of Power Sources* 189 (2009) 547.
- [7] A. K. Mahanta, *Science Horizon* 4-06 (2014) 12.
- [8] E. Pohjalainen, S. Rasanen, M. Jokinen, K. Yliniemi, D. A. Worsley, J. Kuusivaava, J. Juurikivi, R. Ekqvist, T. Kallio, M. Karppinen, *J. of Power Sources* 226 (2013) 134.
- [9] M. Sun, H. Zhong, S. Jiao, H. Shao, L. Zhang, *Electrochimica Acta* 127 (2014) 239.
- [10] Z. Wang, N. Dupre, A. C. Gaillot, B. Lestriez, J. F. Martin, L. Daniel, S. Patoux, D. Guyomard, *Electrochimica Acta* 62 (2012) 77.
- [11] B. Bitsch, J. Dittmann, M. Schmitt, P. Scharfer, W. Schabel, N. Willenbacher, *J. of Power Sources* 265 (2014) 81.
- [12] M. Osinska-Broniarz, A. Martyla, L. Majchrzycki, M. Nowicki, A. Sierczynska, *European J. of Chem.* 7 -2 (2016) 182.
- [13] L. Wei, C. Chen, Z. Hou, and H. Wei, *Scientific Reports* (2016) DOI: 10.1038/srep19583.
- [14] J. Orlenius, O. Lyckfeldt, K. A. Kasvayee, P. Johander, *J. of Power Sources* 213 (2012) 119.
- [15] C. Park, S. B. Park, S. H. Oh, H. Jang, and W. Cho, *Bull. Korean Chem. Soc.* 32-3 (2011) 836.
- [16] Z. Caban-Huertas, O. Ayyad, D. P. Dubal, P. Gomez-Romero, *Sci. Rep.* 6 (2016) 27024; doi: 10.1038/srep27024.
- [17] L. Cheng-Zhang, T. K. F. George, H. M. Kao, *J. of Power Sources* 189 (2009) 155.
- [18] A. Kumar, R. Thomas, N. K. Karan, J. J. S. Arias, M. K. Singh, S. B. Majumder, M. S. Tomar, and R. S. Katiyar, *J. of Nanotechnology* (2009), doi:10.1155/2009/176517, 1-10.
- [19] G. Arnold, J. Garche, R. Hemmer, S. Strobele, C. Vogler, M. Wohlfahrt-Mehrens, *J. of Power Sources* 119-121 (2003) 247.
- [20] A. H. Saputra, L. Qadhayna, A. B. Pitaloka, *Int. J. of Chem. Eng. and Appls.* 5-1 (2014) 36.
- [21] C. Miao, P. Bai, Q. Jiang, S. Sun, X. Wang, *J. of Power Sources* 246 (2014) 232.
- [22] C. M. Julien, K. Zaghbi, A. Mauger and H. Groult, *Adv. in Chem. Eng. and Sci.* 2 (2012) 321.
- [23] A. K. Mahanta, M. Goyal, and D. D. Pathak, *Malaysian Poly. J.* 5-1 (2010) 1-16.
- [24] A. K. Mahanta, I. Dharmasakti and P. K. Pattnayak, *Def. Sci. J.* 57-4 (2007) 435.
- [25] A. K. Mahanta and D. D. Pathak, *Polyurethane Book*, (2012) ISBN 978-953-51-0726-2 229 InTech Open Access Publisher, Croatia (Europe), <http://dx.doi.org/10.5772/47995>.

Biography of Authors:



Dr. Abhay K. Mahanta obtained Ph. D. in Applied Chemistry in the year 2013 from IIT(ISM), Dhanbad, formerly known as Indian School of Mines, Dhanbad. He has about 16 years of research experience in the field of composite propellant science & technology, about three years in development of batteries & explosives for underwater applications. He is presently working as Scientist-E in Naval Science & Technological Laboratory, Visakhapatnam. His current research interest is focused on Li-ion battery fabrication, rheology & modelling, green science & technology, composite materials, and high energy explosives.



Smt. Prerana Priyadarshini received B.Sc (Engg.) in Metallurgy Engineering from Vinobha Bhawe University, Hazaribagh. She is currently working as Scientist-D in Batteries & Explosives Division of Naval Science & Technological Laboratory, Visakhapatnam. Her work profiles are development of batteries for underwater application & development of light aluminum alloy for underwater weapons. Her fields of specialization are heat treatment of aluminum alloys & Li-ion batteries.



Shri Navneet Kumar was born in 1990 at Alinagar (U.P.) and studied diploma in Chemical Engineering from Government Polytechnic, Gorakhpur. His area of interest includes testing and evaluation of explosive devices, fabrication of lithium ion battery cell, testing and performance evaluation of batteries for underwater application.



Dr. T. V. S. L. Satyavani received Ph.D. in Physics in the year 2016 from Andhra University. She has 3 years of research experience in nuclear magnetic resonance, 10 years of experience in fabrication of semiconductor laser diode arrays, and 7 years of experience in Zn-AgO and Li-ion electrochemical power sources. She is currently working as Scientist-F in Batteries & Explosives Division of Naval Science & Technological Laboratory, Visakhapatnam. Her area of research interest includes semiconductor lasers & electrochemical power sources.
